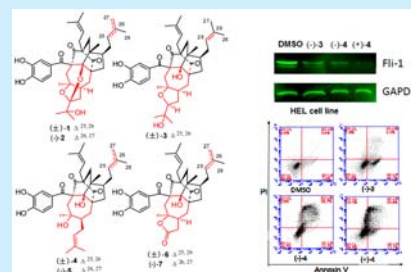


Garmultins A–G, Biogenetically Related Polycyclic  
Acylphloroglucinols from *Garcinia multiflora*Dong Song Tian,<sup>†,§,||</sup> Ping Yi,<sup>†,||</sup> Lei Xia,<sup>†</sup> Xin Xiao,<sup>§</sup> Yi Min Fan,<sup>†</sup> Wei Gu,<sup>†</sup> Lie Jun Huang,<sup>†</sup>  
Yaacov Ben-David,<sup>†</sup> Ying Tong Di,<sup>‡</sup> Chun Mao Yuan,<sup>\*,†</sup> and Xiao Jiang Hao<sup>\*,†,‡</sup><sup>†</sup>The Key Laboratory of Chemistry for Natural Products of Guizhou Province and Chinese Academy of Sciences, Guiyang 550002, P. R. China<sup>‡</sup>State Key Laboratory of Phytochemistry and Plant Resources in West China, Kunming Institute of Botany, Chinese Academy of Sciences, Kunming 650201, P. R. China<sup>§</sup>Guizhou University, Guiyang 550025, P. R. China

## S Supporting Information

**ABSTRACT:** Garmultins A and B (1 and 2), two polycyclic polyprenylated acylphloroglucinols characterized by the coupling of two novel cages, 2,11-dioxatricyclo[4.4.1.0<sup>3,9</sup>]undecane and tricyclo[4.3.1.0<sup>3,7</sup>]decane, along with five biogenetically related analogues (3–7), were isolated from *Garcinia multiflora*. Their structures and absolute configurations were determined by extensive NMR analysis, X-ray crystallography, and electronic circular dichroism calculations. Three compounds were capable of inhibiting oncogene expression and inducing apoptosis in human erythroleukemia cells.



Polycyclic polyprenylated acylphloroglucinols (PPAPs) represent a structurally intriguing class of natural products containing a bicyclo[3.3.1]nonane-2,4,9-trione or bicyclo[3.2.1]octane-2,4,8-trione core that is densely decorated with prenyl, geranyl, or more highly substituted side chains.<sup>1</sup> With fascinating biological profiles and stunningly complex molecular architectures, PPAPs have received considerable attention from the scientific community.<sup>2</sup> The famous *Garcinia*, representing an important source of PPAPs and caged *Garcinia* xanthenes with structurally unique chemical structures and intriguing biological activities, have attracted great interest from the synthetic and pharmacological communities.<sup>3</sup> Specifically, gambogic acid from *Garcinia hanburyi* has been approved for the treatment of lung cancer in phase II clinical trials in China.<sup>4</sup>

In the continuing search for antitumor natural products,<sup>5</sup> garmultins A–G (1–7) (Figure 1), seven new PPAPs, including four pairs of enantiomers (1, 3, 4, and 6) and three optically pure compounds (2, 5, and 7), were isolated from *Garcinia multiflora*. To the best of our knowledge, compounds 1 and 2 represent the first examples of PPAPs characterized by the coupling of two novel cages, 2,11-dioxatricyclo[4.4.1.0<sup>3,9</sup>]undecane and tricyclo[4.3.1.0<sup>3,7</sup>]decane. Two nor-PPAPs (6 and 7) possess an unusual 31,35- $\gamma$ -lactone ring formed through oxidative cleavage of the C-35–C-36 bond in 3. Different precursors formed during the biosynthetic Diels–Alder reactions may be the main reason for the coexistence of racemates and optically pure compounds. Most of the compounds showed moderate cytotoxic activities in vitro against five human cancer cell lines (IC<sub>50</sub> 1.52–9.53  $\mu$ M; Table S11). Compounds (–)-3, (–)-4, and (+)-4 were capable

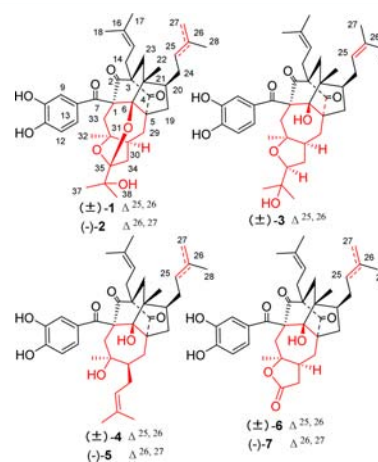


Figure 1. Structures of 1–7.

of inhibiting expression of Friend leukemia virus-induced erythroleukemia-1 (Fli-1), a oncogene of leukemia, and inducing apoptosis of human erythroleukemia (HEL) cells. In this paper, the structural elucidation, plausible biosynthetic pathway, and biological evaluation of the isolated compounds are reported.

Garmultin A (1) was initially obtained as a white powder, and the molecular formula C<sub>38</sub>H<sub>48</sub>O<sub>8</sub> was confirmed by HR-ESI-MS ([M + Na]<sup>+</sup>, *m/z* 655.3236; calcd for C<sub>38</sub>H<sub>48</sub>O<sub>8</sub>Na,

Received: October 6, 2016

Published: November 10, 2016

655.3241) along with  $^1\text{H}$  and  $^{13}\text{C}$  NMR data with 15 degrees of unsaturation. The  $^1\text{H}$  NMR data revealed the presence of eight methyls, two olefinic protons, and a 1,3,4-trisubstituted phenyl ring. The  $^{13}\text{C}$  NMR data along with DEPT experiments showed 38 carbon signals, including eight methyls, seven methylenes, seven methines (five olefinic carbons), and 16 quaternary carbons (five olefinic and three carbonyl carbons). The aforementioned functionalities accounted for nine degrees of unsaturation, and the remaining six degrees of unsaturation indicated **1** to be hexatomic.

The planar structure of **1** was confirmed by 2D NMR spectroscopy (Figure 2) and comparison with the related

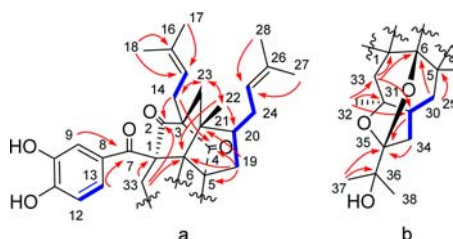


**Figure 2.** Key HMBC (red arrows) and  $^1\text{H}$ – $^1\text{H}$  COSY (blue lines) correlations of **1**.

compound garcimulin A.<sup>5d</sup> The  $^1\text{H}$ – $^1\text{H}$  COSY cross-peaks of  $\text{H}_2$ -14/ $\text{H}$ -23,  $\text{H}_2$ -19/ $\text{H}$ -20/ $\text{H}_2$ -24/ $\text{H}$ -25,  $\text{H}_2$ -29/ $\text{H}$ -30/ $\text{H}_2$ -34, and  $\text{H}$ -12/ $\text{H}$ -13 revealed that **1** features four fragments as highlighted by the bold bonds in Figure 2. Multiple HBMBC correlations (Figure 2a) from  $\text{H}_2$ -14 to C-2, C-3, C-4, and C-23; from  $\text{H}_3$ -22 to C-6, C-20, C-21, and C-23; from  $\text{H}_2$ -19 to C-4, C-5, and C-6; and from  $\text{H}_2$ -33 to C-1, C-2, and C-6 revealed the presence of a caged tricyclo[4.3.1.0<sup>3,7</sup>]decane motif, similar to that of garcimulin A.<sup>5d</sup> From 2D NMR spectra, a 3,4-dihydroxybenzophenone and two prenyl groups could be easily characterized to be present in position C-1, C-3, and C-20, respectively (Figure 2a). In the HMBC spectrum, correlations from  $\text{H}_3$ -32 to C-30, C-31, and C-33; from  $\text{H}_2$ -29 to C-5, C-6, and C-19; and from  $\text{H}_2$ -33 to C-1 and C-6 demonstrated the presence of a seven-membered ring with a methyl at C-31. The linkages of C-34 and C-36 through C-35 could be assigned from the HMBC correlations from  $\text{H}$ -30 and  $\text{H}_2$ -34 to C-35 and from  $\text{H}_3$ -37 and  $\text{H}_3$ -38 to C-35 and C-36. The significantly downfield-shifted signals at  $\delta_{\text{C}}$  91.9 (C-6) and  $\delta_{\text{C}}$  85.8 (C-31), as well as a typical ketal carbon at  $\delta_{\text{C}}$  114.1 (C-35) along with two remaining degrees of unsaturation, indicated that two ether bridges were formed, one between C-6 and C-35 and the other between C-31 and C-35. Consequently, an unprecedented caged 2,11-dioxatricyclo-[4.4.1.0<sup>3,9</sup>]undecane was established (Figure 2b). Taken in concert, the above evidence assigned the planar structure of **1** as displayed in Figure 1.

The relative configuration of **1** was partially deduced by a ROESY experiment (Figure S1), in which cross-peaks from  $\text{H}_3$ -22 to  $\text{H}_2$ -24 and  $\text{H}$ -19 $\beta$  suggested that these groups are cofacial and  $\beta$ -oriented. In addition, ROESY correlations of  $\text{H}$ -19 $\alpha$ / $\text{H}$ -20 and of  $\text{H}$ -30/ $\text{H}_3$ -32 indicated that those groups are cofacial. Unfortunately, because of the lack of sufficient key ROESY correlations, we were unable to assign such a complex scaffold with multiple quaternary carbon atoms. However, crystals suitable for X-ray diffraction could be obtained from acetone. X-ray diffraction analysis, conducted with Mo  $K\alpha$  radiation, not only confirmed the complete structure and relative config-

urations of all asymmetric carbon centers (Figure 3), but also revealed **1** to be racemic with space group  $P\bar{1}$ ,<sup>6</sup> which was

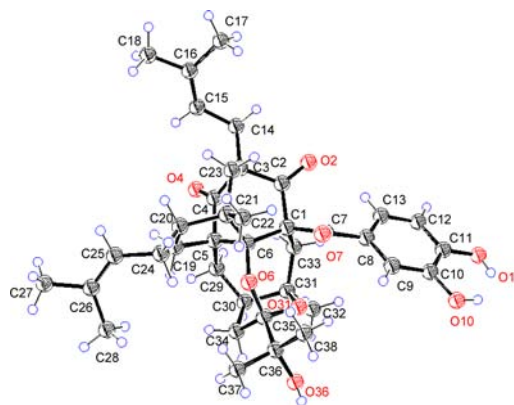


**Figure 3.** X-ray crystallographic structure of **1**.

further supported by the line of the CD spectrum as well as the small optical activity ( $[\alpha]_{\text{D}}^{20}$  –6.3). A subsequent chiral resolution of **1** was performed on a chiral column to yield (+)-**1** and (–)-**1**. The absolute configurations of (+)-**1** and (–)-**1** were assigned by comparing the calculated electronic circular dichroism (ECD) results with the experimental data (Figure 4).<sup>7</sup>

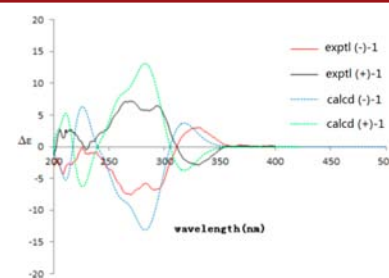
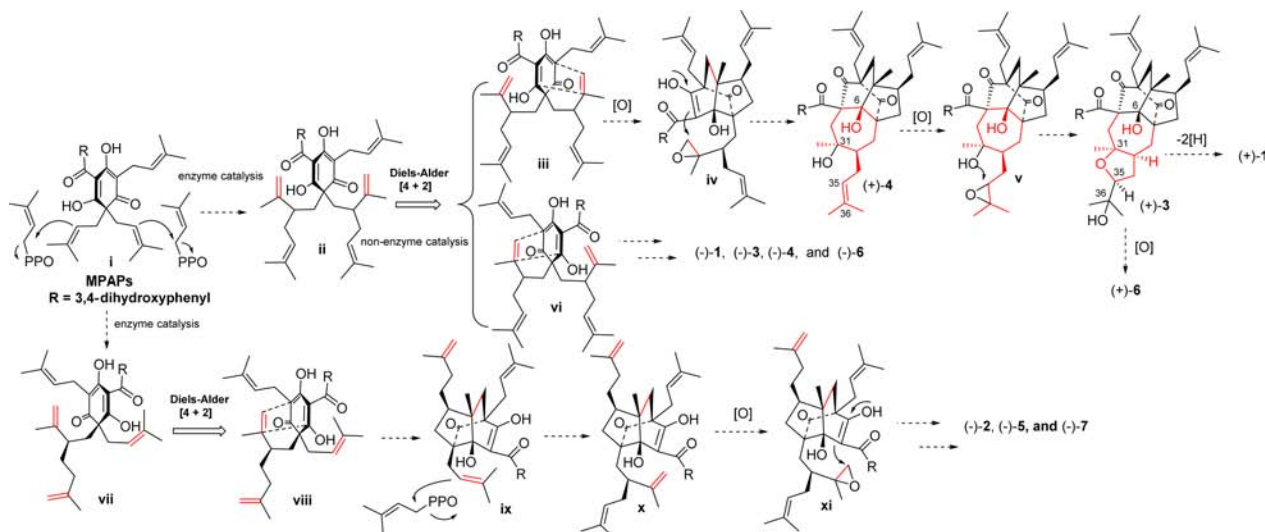


**Figure 4.** Calculated and experimental ECD spectra of (–)-**1** and (+)-**1**.

The results obtained from HR-ESI-MS and NMR analysis of garcmultin B (**2**) indicated that **2** is an analogue of **1**. The only difference is the presence of a terminal double bond in **2** instead of the nonterminal double bond in **1**, which was further confirmed by the HMBC correlations from  $\text{H}_3$ -27 to C-28 and C-25 and from  $\text{H}_3$ -22 to C-20 along with the  $^1\text{H}$ – $^1\text{H}$  COSY cross-peaks of  $\text{H}$ -20/ $\text{H}_2$ -24/ $\text{H}_2$ -25. On the basis of the ROESY spectrum (Figure S1) and similar NMR data, the relative configuration of **2** was assigned to be same as that of **1**. To the best of our knowledge, compounds **1** and **2** are the first examples of PPAPs characterized by the coupling of two novel cages, 2,11-dioxatricyclo[4.4.1.0<sup>3,9</sup>]undecane and tricyclo[4.3.1.0<sup>3,7</sup>]decane, on the backbone.

The structures of the five remaining garcmultins C–G (**3**–**7**) were assigned by NMR analysis and comparison with **1**. Full details of the structural assignment can be found in Tables S2 and S3. It could be presumed that compounds **1**, **3**, **4**, and **6** are racemates on the basis of the lines of the CD spectra as well as the small optical activities. Fortunately, with the help of a CHIRALPAK IC column, the corresponding dextro isomers ((+)-**1**, (+)-**3**, (+)-**4**, and (+)-**6**) and levo isomers ((–)-**1**, (–)-**3**, (–)-**4**, and (–)-**6**) with opposite Cotton effects in the CD spectra and optical activities were resolved (Supporting

Scheme 1. Plausible Biosynthetic Pathways of Garmultins A–G (1–7)



Information, p 21). Interestingly, compounds (–)-2, (–)-5, and (–)-7 with a terminal double bond at the side chain were optically pure, as deduced from the good Cotton curves in the CD spectra and the large optical activities. The absolute configurations of all of the compounds were determined by ECD calculations and comparison with relevant ECD data (Supporting Information, p 33).<sup>7</sup>

In nature, chiral natural products are usually produced in optically pure form, where on occasion nature is known to produce opposite enantiomeric metabolites.<sup>8</sup> To the best of our knowledge, because of a slight difference in the double bond of the side chain, racemic mixtures were produced by the sole species *G. multiflora*. Herein, a putative biosynthetic pathway is proposed to explain this special phenomenon. Presumably, different precursors before the biosynthetic Diels–Alder reactions may be the main reason for the phenomenon.

As shown in Scheme 1, the optically pure and racemic compounds share the same precursor i, which might undergo catalysis by two different enzymes to get ii and vii. As for the racemates, precursor ii undergoes a Diels–Alder reaction on the right or left side of the molecule to produce iii or vi, respectively,<sup>5d</sup> followed by epoxidation and nucleophilic attack of the diketone to give (+)-4 or (–)-4, respectively. The key intermediate (+)-3 or (–)-3 is obtained after epoxidation of a  $\Delta^{35,36}$  double bond and cyclization through nucleophilic attack of a hydroxyl at C-31. Ultimately, (+)-6 or (–)-6 may be derived from (+)-3 or (–)-3 via oxidative cleavage of the C-35–C-36 bond, while (+)-1 or (–)-1 is obtained through cyclization of 3. However, intermediate vii could only undergo an intramolecular Diels–Alder reaction on the left side of the molecule to form viii, which in turn produces (–)-5, (–)-7, and (–)-2 through a series of reactions involving migration of a double bond and a prenylated group, oxidation, and intramolecular cyclization.

All of the isolates were evaluated for their cytotoxic activities against five human tumor cell lines (HL-60, SMMC-7721, A-549, MCF-7, and SW480), and most of compounds exhibited moderate cytotoxic activities with  $IC_{50}$  values ranging from 1.52 to 9.53  $\mu$ M (Table S11).<sup>9a</sup> Interestingly, levo isomers featuring nonterminal double bonds ((–)-1, (–)-3, (–)-4, and (–)-6) exhibited stronger inhibitory activities than the dextro isomers with nonterminal double bonds ((+)-1, (+)-3, (+)-4, and

(+)-6) and the corresponding optically pure compounds with only one terminal double bond ((–)-2, (–)-5, and (–)-7). Compared with (–)-1, (+)-1, and (–)-2, the presence of the additional hydroxy group at C-6 in (–)-3, (+)-3, (–)-4, (+)-4, and (–)-5 was found to improve the cytotoxic activities against the five tumor cell lines. In addition, three PPAPs ((–)-3, (+)-3 and (–)-4) were evaluated for apoptosis and cell-cycle arrest in human erythroleukemia (HEL) cells. The results revealed that the three compounds could induce apoptosis, and two of the compounds, (–)-4 and (+)-4, induced significant G1-phase cell-cycle arrest (Figure 5a, 5b).<sup>9b</sup>

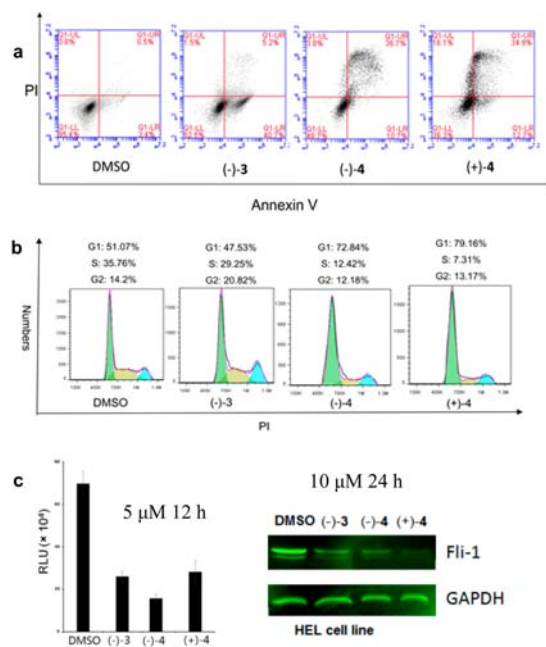


**Figure 5.** (a) Compounds (–)-3, (–)-4, and (+)-4 (10  $\mu$ M for 24 h) induce apoptosis in HEL cells. (b) Effects of compounds (–)-3, (–)-4, and (+)-4 on HEL cell-cycle progression at a concentration of 5  $\mu$ M after 24 h of treatment. (c) Reporter gene and Western blot of inhibition of Fli-1 protein expression of compounds (–)-3, (–)-4, and (+)-4 in HEL cells. GAPDH was used as a loading control.



Fli-1, an ETS transcription factor, has already been reported to be activated in murine erythroleukemia and was found to be overexpressed in various human malignancies, including Ewing's sarcoma.<sup>10</sup> Fli-1, a oncogene, plays a key role in tumorigenesis, and efficient anti-Fli-1 inhibitors may serve as potential anticancer drugs.<sup>11</sup> In order to study the preliminary mechanism of apoptosis and cell-cycle arrest in HEL cells, three PPAPs ((-)-3, (+)-3, and (-)-4) were assessed for inhibition of Fli-1 protein expression in HEL cells. The results revealed that the three PPAPs were capable of inhibiting Fli-1 protein expression, as shown in Figure 5c. This is the first report of PPAPs capable of inhibiting Fli-1 protein expression.

In conclusion, garmultins A–G (1–7), seven highly modified caged polyprenylated acylphloroglucinols (PPAPs) with new skeletons, were isolated from *Garcinia multiflora*. Compounds 1 and 2 represent the first examples of PPAPs characterized by the coupling of two novel cages, 2,11-dioxatricyclo[4.4.1.0<sup>3,9</sup>]-undecane and tricyclo[4.3.1.0<sup>3,7</sup>]decane. Two nor-PPAPs (6 and 7) possess an unusual 31,35- $\gamma$ -lactone ring formed through oxidative cleavage of the C-35–C-36 bond of 3. An unusual phenomenon that racemic mixtures with multiple stereogenic centers were isolated from the same plant has been reported. More importantly, a putative biosynthetic pathway has been proposed to explain this phenomenon. Three PPAPs were found to be capable of inhibiting Fli-1 protein expression and inducing apoptosis in HEL cells.

## ■ ASSOCIATED CONTENT

### Supporting Information

The Supporting Information is available free of charge on the ACS Publications website at DOI: 10.1021/acs.orglett.6b03004.

Experimental details and characterization data (PDF)

X-ray data for compound 1 (CIF)

## ■ AUTHOR INFORMATION

### Corresponding Authors

\*E-mail: haoxj@mail.kib.ac.cn.

\*E-mail: yuanchunmao01@126.com.

### Author Contributions

<sup>†</sup>D.S.T. and P.Y. contributed equally.

### Notes

The authors declare no competing financial interest.

## ■ ACKNOWLEDGMENTS

This research was financially supported by the National Natural Science Foundation of China (81502959), the Natural Science Foundation of Guizhou (QKH J-2015-2106), and the 100 Leading Talents of Guizhou Province (fund for X.J.H.). The science and technology project of Guizhou (QKHT Z-2014-4007). The technology plan of Guizhou (QKH YSZ-2015-4009).

## ■ REFERENCES

- (1) Ciochina, R.; Grossman, R. B. *Chem. Rev.* **2006**, *106*, 3963–3986.
- (2) (a) Biber, N.; Möws, K.; Plietker, B. *Nat. Chem.* **2011**, *3*, 938–942. (b) Richard, J. A.; Pouwer, R. H.; Chen, D. Y. K. *Angew. Chem., Int. Ed.* **2012**, *51*, 4536–4561. (c) Wu, S. B.; Long, C.; Kennelly, E. J. *Nat. Prod. Rep.* **2014**, *31*, 1158–1174.
- (3) (a) Horeischi, F.; Biber, N.; Plietker, B. *J. Am. Chem. Soc.* **2014**, *136*, 4026–4030. (b) Zhang, L.; Feng, J.; Kong, S.; Wu, M.; Xi, Z.; Zhang, B.; Fu, W.; Lao, Y.; Tan, H.; Xu, H. *Cancer Lett.* **2016**, *380*, 447–456. (c) Tang, Y. X.; Fu, W. W.; Wu, R.; Tan, H. S.; Shen, Z. W.; Xu, H. X. *J. Nat. Prod.* **2016**, *79*, 1752–1761. (d) Kan, W. L. T.; Yin, C.; Xu, H. X.; Xu, G.; To, K. K. W.; Cho, C. H.; Rudd, J. A.; Lin, G. *Int. J. Cancer* **2013**, *132*, 707–716. (e) Fu, W. M.; Zhang, J. F.; Wang, H.; Tan, H. S.; Wang, W. M.; Chen, S. C.; Zhu, X.; Chan, T. M.; Tse, C. M.; Leung, K. S.; Lu, G.; Xu, H. X.; Kung, H. F. *Apoptosis* **2012**, *17*, 842–851.
- (4) Shi, X.; Chen, X.; Li, X.; Lan, X.; Zhao, C.; Liu, S.; Huang, H.; Liu, N.; Liao, S.; Song, W.; Zhou, P.; Wang, S.; Xu, L.; Wang, X.; Dou, Q. P.; Liu, J. *Clin. Cancer Res.* **2014**, *20*, 151–163.
- (5) (a) Wang, W.; Liu, H. Y.; Wang, S.; Hao, X. J.; Li, L. *Cell Res.* **2011**, *21*, 730–740. (b) Lv, C.; Yan, X. H.; Tu, Q.; Di, Y. T.; Yuan, C. M.; Fang, X.; Ben-David, Y.; Xia, L.; Gong, J. X.; Shen, Y. M.; Yang, Z.; Hao, X. J. *Angew. Chem., Int. Ed.* **2016**, *55*, 7539–7543. (c) Fang, X.; Di, Y. T.; Zhang, Y.; Xu, Z. P.; Lu, Y.; Chen, Q. Q.; Zheng, Q. T.; Hao, X. J. *Angew. Chem., Int. Ed.* **2015**, *54*, 5592–5595. (d) Fan, Y. M.; Yi, P.; Li, Y.; Yan, C.; Huang, T.; Gu, W.; Ma, Y.; Huang, L. J.; Zhang, J. X.; Yang, C. L.; Li, Y.; Yuan, C. M.; Hao, X. J. *Org. Lett.* **2015**, *17*, 2066–2069.
- (6) Cao, M. M.; Zhang, Y.; Li, X. H.; Peng, Z. G.; Jiang, J. D.; Gu, Y. C.; Di, Y. T.; Li, X. N.; Chen, D. Z.; Xia, C. F.; He, H. P.; Li, S. L.; Hao, X. J. *J. Org. Chem.* **2014**, *79*, 7945–7950.
- (7) (a) Wang, K. B.; Li, D. H.; Hu, P.; Wang, W. J.; Lin, C.; Wang, J.; Lin, B.; Bai, J.; Pei, Y. H.; Jing, Y. K.; Li, Z. L.; Yang, D.; Hua, H. M. *Org. Lett.* **2016**, *18*, 3398–3401. (b) Fang, W.; Ji, S.; Jiang, N.; Wang, W.; Zhao, G. Y.; Zhang, S.; Ge, H. M.; Xu, Q.; Zhang, A. H.; Zhang, Y. L.; Song, Y. C.; Zhang, J.; Tan, R. X. *Nat. Commun.* **2012**, *3*, 1039.
- (8) Finefield, J. M.; Sherman, D. H.; Kreitman, M.; Williams, R. M. *Angew. Chem., Int. Ed.* **2012**, *51*, 4802–4836.
- (9) (a) Yuan, C.-M.; Zhang, Y.; Tang, G.-H.; Li, Y.; He, H.-P.; Li, S.-F.; Hou, L.; Li, X.-Y.; Di, Y.-T.; Li, S.-L.; Hua, H.-M.; Hao, X.-J. *Planta Med.* **2013**, *79*, 163–168. (b) Lim, S.; Kaldis, P. *Development* **2013**, *140*, 3079–3093.
- (10) Li, Y.; Luo, H.; Liu, T.; Zacksenhaus, E.; Ben-David, Y. *Oncogene* **2015**, *34*, 2022–2031.
- (11) (a) Li, Y. J.; Zhao, X.; Vecchiarelli-Federico, L. M.; Li, Y.; Datti, A.; Cheng, Y.; Ben-David, Y. *Blood Cancer J.* **2012**, *2*, e54. (b) Lakhanpal, G. K.; Vecchiarelli-Federico, L. M.; Li, Y. J.; Cui, J. W.; Bailey, M. L.; Spaner, D. E.; Dumont, D. J.; Barber, D. L.; Ben-David, Y. *Blood* **2010**, *116*, 428–436. (c) Ben-David, Y.; Giddens, E. B.; Bernstein, A. *Proc. Natl. Acad. Sci. U. S. A.* **1990**, *87*, 1332–1336.